SF2A 2018
P. Di Matteo, F. Billebaud, F. Herpin, N. Lagarde, J.-B. Marquette, A. Robin, O. Venot (eds)

REVIEW ON HIGH-MASS STAR FORMATION

F. Louvet[1]

Abstract. Massive star formation is a key astrophysical process. Despite representing only ∼1% of the Galactic stellar population, massive stars ($M_\star > 8\ M_\odot$) input more energy and momentum into the interstellar medium than the other 99% combined. In other words, massive stars govern the energy budget of galaxies and regulate their evolution across the Universe. However, many unknowns still remain, especially regarding the earliest stages of their formation. In this short review, I will present three cornerstones in the process of high-mass star formation: i) how to form the hyper-dense, hyper-massive molecular clouds in which massive stars preferentially form ii) how these molecular clouds form high mass stars (dynamical versus quasi-static evolution) and iii) how to circumvent the radiation pressure issue at small scale.

Keywords: Star-formation, Massive star, Cloud-cloud collision

1 Introduction

Star formation is a fundamental process in astrophysics, the physical mechanisms of which have been studied for decades (see e.g., reviews by André et al. 2014, Krumholz 2015). On large scales, it regulates the evolution of galaxies, while on small scales it determines the initial conditions for the formation of planetary systems. As of now, most of our knowledge is concentrated on the formation of stars of a few solar masses. If galaxies' total stellar mass is dominated by low-mass stars, their energy budget is exclusively controlled by the enormous luminosity and powerful feedback of massive stars. High-mass stars, also called OB stars, have luminosities larger than $10^3\ L_\odot$, spectral types of B3 or earlier, and stellar masses from 8 $M_\odot$up to possibly ∼300 $M_\odot$(Crowther et al. 2010). Despite their importance, the mechanisms leading to the formation of high-mass stars remain a mystery in many aspects. From the theoretical point of view, low-mass star formation models are not directly transposable since they do not provide accretion rates in line with what is necessary for high-mass star formation. From the observational point of view, until the recent raise of large interferometers such as ALMA, little was known about the formation of massive stars due to their scarcity, and remoteness. Unlike the case for low-mass stars (see, e.g., Shu et al. 1987; André et al. 2000), there is no observational evolutionary sequence that is firmly established for high-mass star formation. High-mass stars are observed to form within massive dense cores (MDCs) that are cloud corpuscles of ∼100 $M_\odot$within ∼0.1 pc. These MDCs themselves are preferentially observed in hyper-massive and hyper-dense molecular clouds. Many mysteries exist in the process of high-mass star formation and it goes beyond the scope of the present proceeding to address all of them. Instead, this review discusses three major issues of high-mass star formation, each one taking place at a peculiar physical scale. The section 2 discusses of the formation of the hyper-massive and hyper-dense molecular clouds in which massive stars form. The section 3 focuses on the MDCs, the evolution of which strongly differs depending on the theoretical model one assumes. I will present these models and the observational constraints obtained so far. The section 4 discusses how to circumvent the radiation pressure problem at the scale of individual protostar. Finally, the section 5 presents our conclusion, together with the empirical model for massive star formation that was presented in Tigé et al. (2017) and Motte et al. (2018).

[1] Facultad de ciensas físicas y matemáticas, Universidad de Chile, Santiago, Chile; flouvet@das.uchile.cl

2 Formation of hyper-massive and hyper-dense molecular clouds

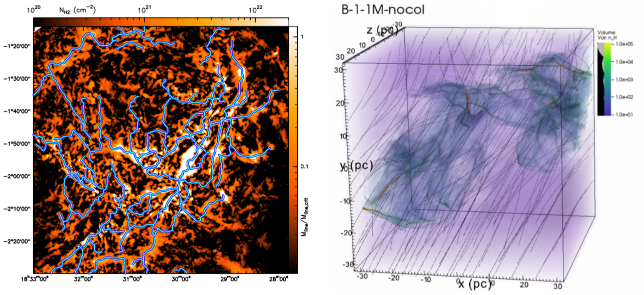

Fig. 1: **Left:** network of filaments in the Aquila low-mass star forming cloud complex on the Herschel column density map; the overplotted blue skeleton marks the crests of the filaments selected with the DisPerSE algorithm (extracted from Könyves et al. 2015). **Right:** Numerical simulation of a non-collisional molecular cloud (extracted from Wu et al. 2017).

The numerical models of e.g. Wu et al. (2017) show that the clouds initialized with a supersonic turbulent velocity field form a network of filaments. They show that these clouds evolve in a relatively quiescent manner, driven by the initial turbulence and interplay of self-gravity and magnetic fields. The stars form dispersed throughout the molecular cloud complex and on the crest of filaments. These models with low dynamics (non-collisional) mimic very well the features observed toward low-mass star forming regions. The figure 1 displays side by side the result of a numerical simulation with low dynamics (right panel, extracted from Wu et al. 2017) and an *Herschel* observation of the Aquila star-forming region (left panel, extracted from Könyves et al. 2015). In both plots there is a network of filaments, with cores forming on the crest of the filaments.

On the other hand the structure and kinematics of massive clouds are extreme relative to those of low-mass star-forming regions. One striking example is the prototypical DR21 hyper-dense structure, located at the heart of the CygX-North cloud (Schneider et al. 2010; Hennemann et al. 2012, see Fig. 2-left). Looking at the morphology of DR21, there is not a network of filament as in the low-mass star forming regime but one hyper-dense cloud that dominates its environment. Some secondary filaments that do not form stars are also observed. They are connected to the central hyper-dense cloud, and dynamical studies have shown that the gas in these secondary filaments flows toward the potential well of the dominating structure (e.g., Schneider et al. 2010). Numerically, it has been demonstrated by Wu et al. (2017) that a large-scale shock between two clouds could reproduce the features typical of the massive star formation regions. The figure 2-right shows the result of the numerical simulation of such a *cloud-cloud collision*.

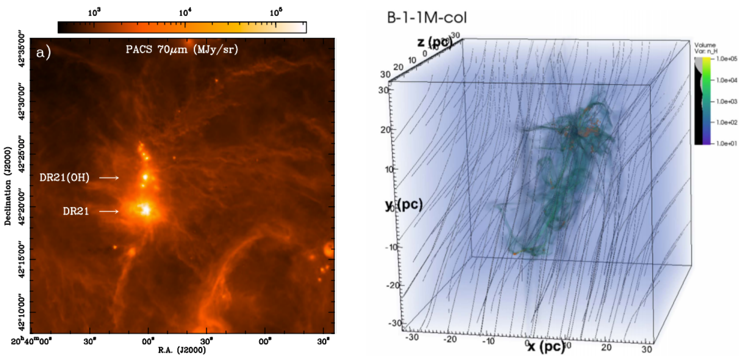

Fig. 2: **Left:**: *Herschel* map of the DR21 environment showed at 70 μm (extracted from Hennemann et al. 2012). **Right:** Numerical simulation of a cloud-cloud collision (extracted from Wu et al. 2017).

Interestingly, such cloud-cloud collision would provoke low-velocity shocks, and thus large-scale emission of molecules enhanced in shocks. Large-scale SiO emission has been found along several hyper-massive molecular clouds (see, Jiménez-Serra et al. 2010; Nguyen-Lu'o'ng et al. 2013; Sanhueza et al. 2013; Duarte-Cabral et al. 2014). Nevertheless the SiO is mostly known to trace high-velocity shocks associated with the outflows driven by accreting protostars (e.g., Gueth et al. 1998; Dutrey et al. 1997). The observational studies mentioned above lacked the angular resolution to dissociate the SiO emission associated with the proto-stars embedded in the molecular cloud from a potential large-scale homogenous emission. Therefore the interpretation of the large-scale SiO emission as being due to a cloud-cloud collision was putative. Louvet et al. (2016b) observed the large-scale SiO emission ($\simeq$5 pc) of the W43-MM1 hyper-dense molecular cloud with the IRAM/PdBI interferometer and managed for the first time to resolve the outflows. The Figure 3-right shows the integrated intensity map of the SiO (2→1) emission. The red and blue contours highlight the integrated high-velocity emissions of the SiO molecular line, betraying the presence of outflows. Most of the SiO emission is not associated with these outflows. Moreover, the SiO emission has a narrow line profile ($\sim$6 km s^{-1}) at positions deprived of outflows (e.g., positions 3 and 5 on Figure 3), which betrays a low-velocity shock. One difficulty with this interpretation is that the SiO was thought to form in the gas phase after liberating the Si from the refractory core of the dust grain. But it takes shock velocity of at least 20 km s^{-1} to erode the core of the dust grain. It is then necessary to consider that a fraction of the Si abundance is located outside of the dust grain. To test this view we ran a grid of shock model dedicated to the W43-MM1 hyper-dense molecular cloud with the Paris-Durham shock model (Flower & Pineau des Forêts 2015). The Figure 3-left displays the emission of SiO reached in the model as a function of the shock velocity for a set of models where we considered the fraction of the Si located outside of the core of the dust grain as equals to 1% and 10%, and where we consider the irradiation factor equals to $G_0 = 0$ and $G_0 = 1$. We show that such models, where a fraction of the abundance of the Si is placed outside of the core of the dust grain can reproduce the emissions of SiO observed in W43-MM1 for shock velocities from 9 km s^{-1} to 12 km s^{-1}. Therefore Louvet et al. (2016b) proved that a cloud-cloud collision was occurring in the W43-MM1 high-density cloud and that the subsequent low-velocity shock can liberate SiO from the dust grain.

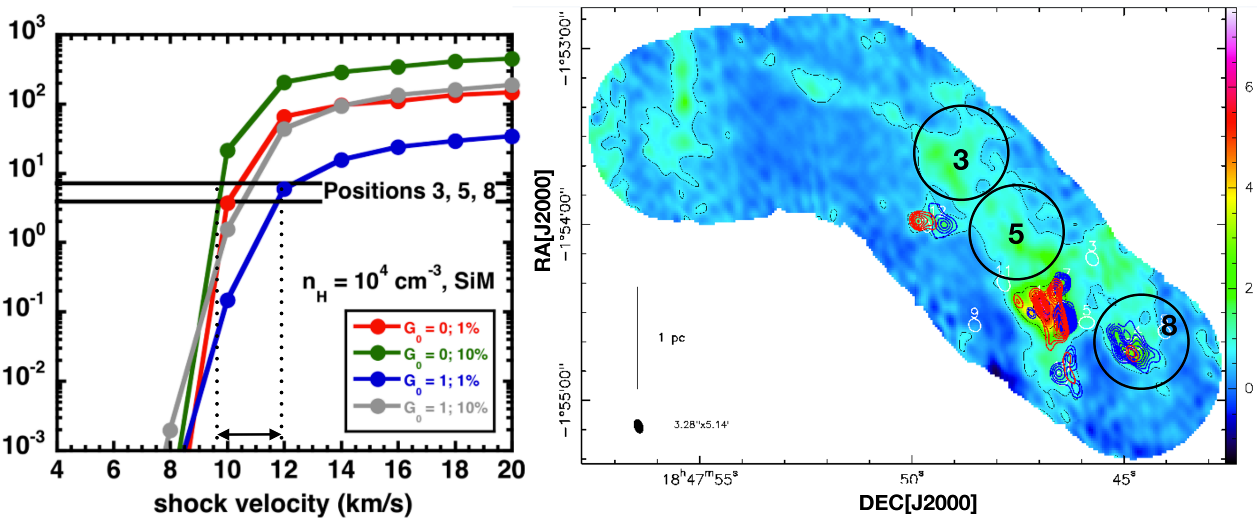

Fig. 3: **Left:** Integrated intensity of the SiO(2→1) transition against the shock velocity calculated for a preshock density of $n_{\rm H} = 10^4$ cm^{-3} (coloured symbols), and compared to the observations (thick, horizontal black lines corresponding to positions 3, 5, and 8). The color code is indicated in the panels, where the G_0 (= 0 or 1) value and fraction of preshock free silicon (=1 or 10%) is shown for each model. **Right:** Extended SiO emission toward the W43-MM1 ridge. SiO(2→1) maps, integrated from 80 km s^{-1} to 120 km s^{-1}, were obtained by merging the IRAM/PdBI and the IRAM/30m data sets.

3 Massive dense cores

Two main theoretical scenarios have been proposed to explain the formation of high-mass stars: *(1)* monolithic collapse of a MDC supported by supersonic turbulent pressure (e.g., McKee & Tan 2002; Krumholz et al. 2007) or *(2)* colliding flows initiated by competitive accretion or cloud formation (e.g., Bonnell et al. 2004; Bonnell & Bate 2006; Vázquez-Semadeni et al. 2009). These two scenarios lead to distinct characteristics for the initial stages of high-mass star formation. The first family of models supposes the existence of starless MDCs that are supported by a high-degree of micro-turbulence ($\sigma \sim$1.7-2 km s^{-1}, Krumholz et al. 2007). The MDCs contract quasi-statically to become high-mass pre-stellar cores ($\sim$30 M$_\odot$ for a radius of $\sim$0.03 pc) before becoming proto-stellar cores. Here, "core" names a gaseous structure of $\sim$0.03 pc (Bontemps et al. 2010; Zhang et al. 2014; Palau et al. 2015) that will collapse to form a single star or a small N-tuple binary system. Hence, quasi-static models predict the existence of one, or a few, high-mass pre-stellar cores in the starless MDCs. In the second family of models, high-mass pre-stellar cores never develop. The starless MDCs fragment into a cluster of low-mass cores with initial masses of the order of the Jeans mass. When favourably located at the centres of MDCs' gas reservoir, the low-mass pre-stellar cores attract gas from further distances and eventually become high-mass protostars.

High-resolution studies have been performed with (sub)millimeter interferometers with the aim of identifying pre-stellar cores and protostars within MDCs (see Rathborne et al. 2007; Swift 2009; Zhang et al. 2009; Busquet et al. 2010; Bontemps et al. 2010; Pillai et al. 2011; Wang et al. 2011; Zhang & Wang 2011; Beuther et al. 2013; Lee et al. 2013; Tan et al. 2013; Wang et al. 2014; Louvet et al. 2014; Cyganowski et al. 2014; Duarte-Cabral et al. 2014; Fontani et al. 2016; Louvet et al. 2016b,a; Kong et al. 2017; Palau et al. 2018; Louvet et al. 2018; Csengeri et al. 2018; Nony et al. 2018). These attempts revealed either that they were proto-stellar in nature when observed at high resolution (e.g. Duarte-Cabral et al. 2013), or filled with low-mass pre-stellar cores (see e.g., Tan et al. 2013; Kong et al. 2017). In total, only five high-mass pre-stellar core candidates have been reported:

- The pre-stellar candidate CygX-N53-MM2 ($\sim$25 $M_\odot$ within 0.025 pc) of Duarte-Cabral et al. (2014); however, owing to the confusion with the neighbour CygX-N53-MM1, it is hard to exclude that CygX-N53-MM2 is driving outflows.

- The pre-stellar candidate G11.92-0.61-MM2 ($>30 M_\odot$ within 0.01 pc) of Cyganowski et al. (2014) but the lack of (sub)millimeter molecular line emissions casts doubt about its belonging to the Milky Way.

- The pre-stellar candidate G11.11-P6-SMA1 ($\sim$30 $M_\odot$ within 0.02 pc) of Wang et al. (2014). This source seems deprived of outflows but a spectral survey of this target is necessary to determine if it hosts a hot core.

- The source G028CA9 ($\sim$70 $M_\odot$ within 0.04 pc) of Kong et al. (2017) but this source still lacks of shock tracer analysis to address if it is driving outflows. Also, according to the authors, it shows complex kinematics potentially indicative of two merging structures.

- The source W43-MM1-6 by Nony et al. (2018). They found a massive core of 56 $M_\odot$within 1300 au. This target is deprived of outflow and its spectrum does not show numerous complex organic molecule emission as commonly observed towards hot cores. A follow up analysis of molecular emission line features is ongoing (Mollet et al. in prep).

Therefore, although many regions have been studied, very few high-mass pre-stellar core candidates have been reported, which proves that, if they exist, they are very elusive. According to the detailed statistical study of Tigé et al. (2017), high-mass prestellar cores should live for less than 1-7 $\times 10^4$ years - near their free-fall time. Indeed, the free-fall time of a putative high-mass prestellar core of full-volume averaged densities equivalent to that of high-mass protostars, $< \mathrm{n_{H2}} >_{\mathrm{full}} \sim 1.3 \times 10^6$ cm^{-3}, is $\tau_{ff-prestellar} \sim 3 \times 10^4$ years. This statistical lifetime of high-mass prestellar cores has two consequences: *(i)* high-mass prestellar cores cannot form quasi-statically over several free-fall times as was assumed by McKee & Tan (2002), else the observational studies should have discovered them and *(ii)* if high-mass prestellar cores exist, they must quickly assemble their mass and collapse in a time near the free-fall time, such that current high-resolution studies could still have failed in detecting them. The alternative interpretation of short lifetimes for the high-mass prestellar phase is that high-mass prestellar cores simply do not exist as small ($\sim$0.02 pc) condensations, isolated from their environment. Both the lifetime of high-mass protostars and the infalling gas observed down to the protostellar scale indeed invoke that high-mass stars form while still strongly interacting with their surroundings. First, the high-mass protostellar lifetime suggests that the collapse starts within a low-mass prestellar core and continues within a protostellar envelope, which grows from low to high mass (e.g., Tigé et al. 2017). Moreover, high-mass stars form into infalling clumps at 1-pc scales, whose global collapse drives inflowing gas streams toward protostars at 0.01-pc scales (e.g., Schneider et al. 2010; Csengeri et al. 2011). This evolutionary scenario corresponds to an extension of the competitive accretion model, when accretion through inflowing gas streams driven by gravity replaces the Bondi-Hoyle accretion (Smith et al. 2009). In this scenario, high-mass protostars would then be fed from the gas of their surrounding MDCs/clumps, following the clump-fed scenario of protostellar accretion, in contrast with the the core-fed scenario of low-mass protostellar accretion and of the McKee & Tan (2002) model.

4 Massive disks around massive protostars

For long, the theoretical community tried and solve the UV radiation pressure problem (Wolfire & Cassinelli 1987). This problem is that stars reaching a few 10 $M_\odot$ and a few 10^3 $L_\odot$ were supposed to develop a pressure barrier halting further accretion. Most recent 3D modelling mostly solved this problem by showing that equatorial accretion can continue for ionizing protostar embryos (e.g., Kuiper et al. 2010). The figure 4 shows a schematic view of an isotropic accretion (such as a Bondi-Hoyle accretion) on the left panel and an accretion via an axially symmetric circumstellar disk on the right panel as it is often observed toward low-mass protostars (e.g., Louvet et al. 2016a, 2018). The latter numerical simulations are able to form stars with masses of up to 40-140 $M_\odot$ thanks to this non-spherical accretion, improved radiation transfer, and feedback effects such as heating and ionization (e.g., Kuiper et al. 2010). Modelling the formation of higher mass stars remain a challenge since photoionizing radiation will blow out the polar regions of a rotating accretion flow around an accreting star once its mass reaches $\sim$ 50-100 $M_\odot$, and will thereafter go on to photoevaporate the disk. This process will halt accretion at a mass of $\sim$150 $M_\odot$ (Krumholz 2015).

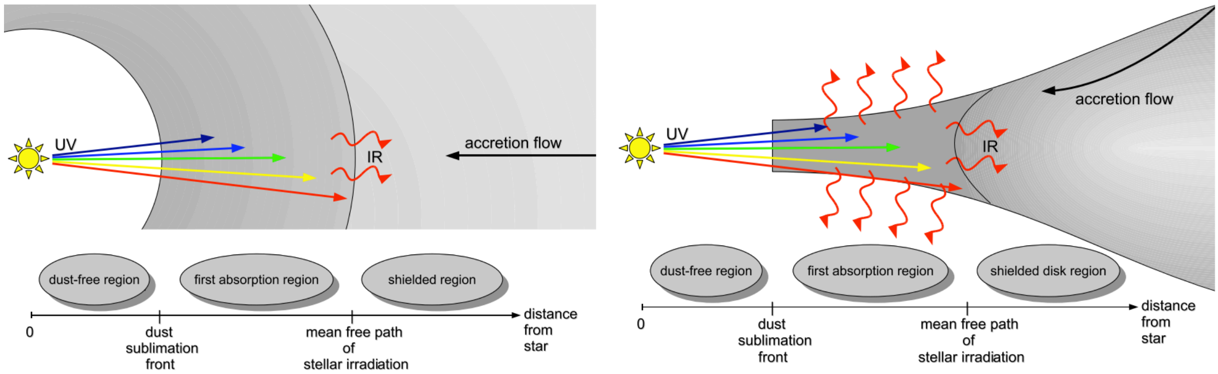

Fig. 4: **Left:** Schematic view of the radiative forces onto the accretion flow in spherical symmetry. **Right:** Schematic view of the“UV”- and “IR”-component of the radiation pressure acting in an axially symmetric circumstellar disk geometry (figures extracted from Kuiper et al. 2010).

5 Conclusions

Figure 5 illustrates the evolutionary scheme we proposed in Motte et al. (2018) for the formation of high-mass stars. This empirical scenario is based on observational constraints and qualitatively recalls the global hierarchical collapse and clump-fed accretion scenarios. Despite the large binary fraction of high-mass stars, the present scenario do not include yet their formation because of the lack of observational constraints.

1. High-mass stars form in molecular complexes hosting massive clouds and often OB clusters. Parsec-scale massive clumps/clouds called ridges and hubs are the preferred, if not the only, sites of high-mass star formation. Their infall velocity and density structure suggest that ridges/hubs undergo a global but controlled collapse.

2. At first, IR-quiet MDCs are 0.1-pc massive cloud fragments, which host low-mass prestellar cores. They represent the starless MDC phase lasting for about one free-fall time ($\sim 10^5$ years.)

3. At the MDC center, low-mass prestellar cores become protostars with growing mass and not high-mass prestellar cores. The global collapse of ridges/hubs generates gas flow streams, which simultaneously increase the mass of MDCs and, on 0.02-pc scales, of their hosted protostar(s). Typically, in $\sim 10^5$ years, two high-mass protostars form in 0.1-pc MDCs.

4. When inflowing gas streams are efficient to reach and feed the low-mass protostellar cores, the latter become IR-quiet high-mass protostars. They have 0.02-pc sizes and super-Jeans masses but still only harbour low-mass (<8 $M_\odot$) stellar embryos. Their accretion rates are strong; they drive outflows and power hot cores.

5. When stellar embryos reach 8 $M_\odot$, their luminosity sharply increases, and high-mass protostars become IR-bright. Their hot cores grow in size, and they soon develop HCHII regions quenched by infalling gas or localized toward photoevaporating disks.

6. Stellar embryos have increasing UV fields that develop HII regions, which, along with other processes including outflows and winds, slow and eventually stop gas accretion toward the newborn star. This terminates the main accretion phase.

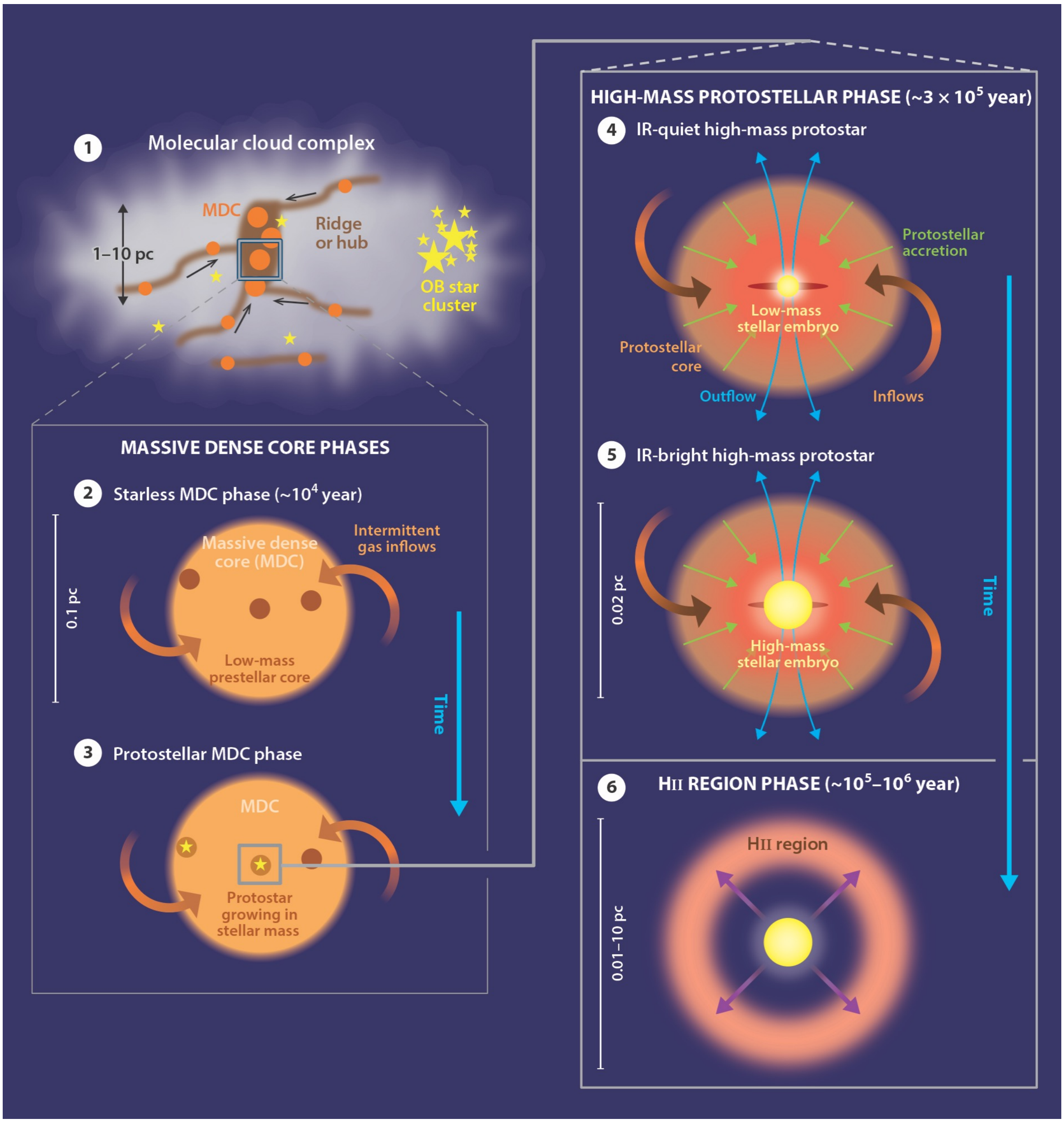

Fig. 5: Schematic evolutionary diagram proposed for the formation of high-mass stars, see text.

The past fifteen years have seen an increasing interest in approaching the issue of the formation of high-mass stars and massive clusters from both the theoretical and observational sides. High-mass star-formation scenarios currently undergo a change of paradigm, in which this process is no longer quasi-static but simultaneously evolves with both cloud and cluster formation. The lifetimes of high-mass protostars and the lack of high-mass ($\sim$0.02 pc-scale) prestellar cores are consistent with the large dynamics of their hosted hyper-dense molecular clouds and MDCs on $\sim$0.1-1-pc scales. With the multiplication of observational studies with ALMA, the issues associated with the lack of angular resolution and the lack of statistics are about to be solved.

References

André, P., Di Francesco, J., Ward-Thompson, D., et al. 2014, Protostars and Planets VI, 27
André, P., Ward-Thompson, D., & Barsony, M. 2000, Protostars and Planets IV, 59
Beuther, H., Linz, H., Tackenberg, J., et al. 2013, A&A, 553, A115
Bonnell, I. A. & Bate, M. R. 2006, MNRAS, 370, 488
Bonnell, I. A., Vine, S. G., & Bate, M. R. 2004, MNRAS, 349, 735
Bontemps, S., Motte, F., Csengeri, T., & Schneider, N. 2010, A&A, 524, A18
Busquet, G., Palau, A., Estalella, R., et al. 2010, A&A, 517, L6
Crowther, P. A., Schnurr, O., Hirschi, R., et al. 2010, MNRAS, 408, 731
Csengeri, T., Bontemps, S., Schneider, N., Motte, F., & Dib, S. 2011, A&A, 527, A135
Csengeri, T., Bontemps, S., Wyrowski, F., et al. 2018, A&A, 617, A89
Cyganowski, C. J., Brogan, C. L., Hunter, T. R., et al. 2014, ApJ, 796, L2
Duarte-Cabral, A., Bontemps, S., Motte, F., et al. 2014, A&A, 570, A1
Duarte-Cabral, A., Bontemps, S., Motte, F., et al. 2013, A&A, 558, A125
Dutrey, A., Guilloteau, S., & Bachiller, R. 1997, A&A, 325, 758
Flower, D. R. & Pineau des Forêts, G. 2015, A&A, 578, A63
Fontani, F., Commerçon, B., Giannetti, A., et al. 2016, A&A, 593, L14
Gueth, F., Guilloteau, S., & Bachiller, R. 1998, A&A, 333, 287
Hennemann, M., Motte, F., Schneider, N., et al. 2012, A&A, 543, L3
Jiménez-Serra, I., Caselli, P., Tan, J. C., et al. 2010, MNRAS, 406, 187
Kong, S., Tan, J. C., Caselli, P., et al. 2017, ApJ, 834, 193
Könyves, V., André, P., Men'shchikov, A., et al. 2015, A&A, 584, A91
Krumholz, M. R. 2015, in Astrophysics and Space Science Library, Vol. 412, Very Massive Stars in the Local Universe, ed. J. S. Vink, 43
Krumholz, M. R., Klein, R. I., & McKee, C. F. 2007, ApJ, 656, 959
Kuiper, R., Klahr, H., Beuther, H., & Henning, T. 2010, ApJ, 722, 1556
Lee, K., Looney, L. W., Schnee, S., & Li, Z.-Y. 2013, ApJ, 772, 100
Louvet, F., Dougados, C., Cabrit, S., et al. 2016a, A&A, 596, A88
Louvet, F., Dougados, C., Cabrit, S., et al. 2018, ArXiv e-prints
Louvet, F., Motte, F., Gusdorf, A., et al. 2016b, A&A, 595, A122
Louvet, F., Motte, F., Hennebelle, P., et al. 2014, A&A, 570, A15
McKee, C. F. & Tan, J. C. 2002, Nature, 416, 59
Motte, F., Bontemps, S., & Louvet, F. 2018, ARA&A, 56, 41
Nguyen-Lu'o'ng, Q., Motte, F., Carlhoff, P., et al. 2013, ApJ, 775, 88
Nony, T., Louvet, F., Motte, F., et al. 2018, ArXiv e-prints
Palau, A., Ballesteros-Paredes, J., Vázquez-Semadeni, E., et al. 2015, MNRAS, 453, 3785
Palau, A., Zapata, L. A., Román-Zúñiga, C. G., et al. 2018, ApJ, 855, 24
Pillai, T., Kauffmann, J., Wyrowski, F., et al. 2011, A&A, 530, A118
Rathborne, J. M., Simon, R., & Jackson, J. M. 2007, ApJ, 662, 1082
Sanhueza, P., Jackson, J. M., Foster, J. B., et al. 2013, ApJ, 773, 123
Schneider, N., Csengeri, T., Bontemps, S., et al. 2010, A&A, 520, A49
Shu, F. H., Adams, F. C., & Lizano, S. 1987, ARA&A, 25, 23
Smith, R. J., Longmore, S., & Bonnell, I. 2009, MNRAS, 400, 1775
Swift, J. J. 2009, ApJ, 705, 1456
Tan, J. C., Kong, S., Butler, M. J., Caselli, P., & Fontani, F. 2013, ApJ, 779, 96
Tigé, J., Motte, F., Russeil, D., et al. 2017, A&A, 602, A77
Vázquez-Semadeni, E., Gómez, G. C., Jappsen, A.-K., Ballesteros-Paredes, J., & Klessen, R. S. 2009, ApJ, 707, 1023
Wang, K., Zhang, Q., Testi, L., et al. 2014, MNRAS
Wang, K., Zhang, Q., Wu, Y., & Zhang, H. 2011, ApJ, 735, 64
Wolfire, M. G. & Cassinelli, J. P. 1987, ApJ, 319, 850
Wu, B., Tan, J. C., Christie, D., et al. 2017, ApJ, 841, 88
Zhang, B., Moscadelli, L., Sato, M., et al. 2014, ApJ, 781, 89
Zhang, Q. & Wang, K. 2011, ApJ, 733, 26
Zhang, Q., Wang, Y., Pillai, T., & Rathborne, J. 2009, ApJ, 696, 268